The combined use of millimetre wave imaging and acoustic emission for the damage investigation of glass fibre reinforced polymer composites

Kalliopi-Artemi Kalteremidou[1], Ali Pourkazemi[2], Youssef El Idrissi[1], Youssef Morabet[1], Guoqiang He[2], Johan Stiens[2], Lincy Pyl[1] and Danny Van Hemelrijck[1]
1 Department of Mechanics of Materials and Constructions, Vrije Universiteit Brussel, BE-1050 Brussels, Belgium, e-mail: Kalliopi-Artemi.Kalteremidou@vub.be
2 Department of Electronics and Informatics, Vrije Universiteit Brussel, BE-1050 Brussels, Belgium, e-mail: jstiens@etrovub.be

Abstract

In this study, different Non Destructive Techniques, like Millimetre Wave spectroscopy, Acoustic Emission, Digital Image Correlation and online microscopy are combined in order to monitor the damage of a Glass Fibre Reinforced Epoxy composite material under static loads. The capabilities of all these techniques are studied and combined in order to investigate the potential of using them as damage monitoring tools.

1. Introduction

During the last years, a rapid increase in the use of fibre reinforced polymer composite materials at various applications has been recorded mainly due to their high specific strength and specific stiffness. Composites are anisotropic materials and their damage development depends on various parameters. Monitoring of this damage with respect to all these parameters is of great importance if full characterization of the materials is necessary. Moreover, monitoring the damage of composites under different circumstances in lab conditions can be used as damage predictive tool in real applications and for the establishment of damage criteria.
In order to be able to understand how the different parameters influence the damage of materials and to be able to predict their damage in real applications, Non-Destructive Techniques (NDTs) are usually used. Acoustic Emission (AE) is a commonly used technique which allows us to realize the damage of a material by interpreting the elastic waves that generate within the material when it undergoes irreversible changes. AE is a powerful technique and by using relatively simple equipment, damage can be detected and characterized during loading. (1)-(4) However, interpretation of the AE data is not so simple in the case of composite materials and most of the times it can provide qualitative but not quantitative conclusions. Ideally, the AE activity should be directly compared with a method that provides a more physical overview of the damage state of the material. One of the relatively recently developed NDTs in the field of material engineering is the Millimetre Wave (MMW) Spectroscopy which is an emerging method based on electromagnetic wave radiation within the 30 to 300 GHz band, enabling non-invasive, non-ionizing and non-contact examination of dielectric

materials, like Glass Fibre Reinforced Polymers (GFRPs). (5) The use of this method for the damage investigation of materials (6) is gaining more and more interest but it is still quite unexplored especially in the damage investigation of composite materials.
In literature, MMW is used for the damage investigation in composite materials, especially for the examination of the fibre content, the presence of voids and the development of delaminations. (7)-(8) Efforts have also been reported on the use of GHz radiation for the inspection and quality control of GFRPs after manufacturing. (9)-(11) The combination of MMW with other NDTs, like infrared thermography for the damage investigation of composites due to impact has also proved to be quite promising. (12)
In our work, a new research effort is performed by combining AE and MMW together with other NDTs in order to examine the damage of GFRP coupons under static tensile loads. The potential of combining these NDTs for the damage characterization is discussed and preliminary results are reported. The MMW technique used in our research combines various advantages in comparison to other NDTs, like high resolution, high defect-detection and positioning capability, owing to its high penetration capability. The use of these two techniques is combined with the use of Digital Image Correlation (DIC) for capturing the surface strains on the material and an online microscope allowing us to measure the damage occurring through the thickness of the flat specimens under tensile loads.

2. Materials and equipment

The material used in this study was a pre-preg GFRP consisting of an epoxy resin and unidirectional glass fibres. The material was provided by c-m-p company and GFRP plates were manufactured with hand lay-up and were cured in an autoclave at 6 bar pressure and 120^{o} C temperature for four hours.
For this initial study, a cross-ply lay-up was selected to investigate the potential of using different NDTs for damage monitoring. Specifically, cross-ply plates with a lay-up of $[(90^{o})_2/(0^{o})_2]_s$ were manufactured and tested. After the curing process of the plates, specimens were cut with dimensions according to the ASTM D3039 standard with total length of 250 mm, thickness varying from 1.6 mm to 1.7 mm and width of 25 mm. All the specimens were tabbed in a length of 50 mm using the same GFRP material. All tests were performed on a MTS servo-hydraulic machine with a load cell of 100 kN capacity. The static tests were performed displacement controlled with a rate of 1 mm/min. At least 3 repetitions for each test case were performed.
Monitoring of the mechanical response and the damage was performed using different NDTs. The acoustic activity during the tests was measured using an eight-channel DiSP system by Physical Acoustics. Two piezoelectric transducers (Pico) with a broadband response and maximum sensitivity at 450 kHz were mounted on the specimen using vaseline. Preamplifiers were used to amplify the signals with a uniform gain of 40 dB and a 35 dB threshold was applied to filter out the noise of the mechanical system.
The strains during testing were measured using a 50 mm extensometer. At the same time, a DIC system VIC-3D by Correlated Solutions with two camera lenses was used in order to obtain the full-field strain maps during testing through triangulation of the two cameras. A random black-white speckle pattern was applied on the specimens using aerosol paint and by capturing regular images of the surface of the specimens, the in-plane strains of the specimens were calculated.

At the same time, a Leica microscope was mounted on the frame of the MTS system. By this, monitoring of the through-thickness damage of the material during testing was possible. For this reason, the tests were interrupted at specific steps and monitoring of the through-thickness damage along the specimens was possible without unmounting the specimens from the machine.
Last but not least, a MMW set-up operating in reflection and transmission mode was used. Specifically, a spectroscopy method by means of sweeping millimetre waves from 50 to 70 GHz was applied. In addition, four parabolic mirrors were used to converge the antennas beam as well as to provide ambient isolation. Moreover, in order to increase the resolution and to gain higher sensitivity, the interferometry phenomena have been increased using a structure of double glasses with a certain air gap working as a resonator. (13) The resonator was placed between two parabolic mirrors with the front side of the specimen laying on the back wall of the resonator. A directional coupler at the transducer part allowed recording of the reflected signal while the receiver was used to record the transmitted signal.
In Figure 1 the set-up used for testing and the MMW equipment used are shown.

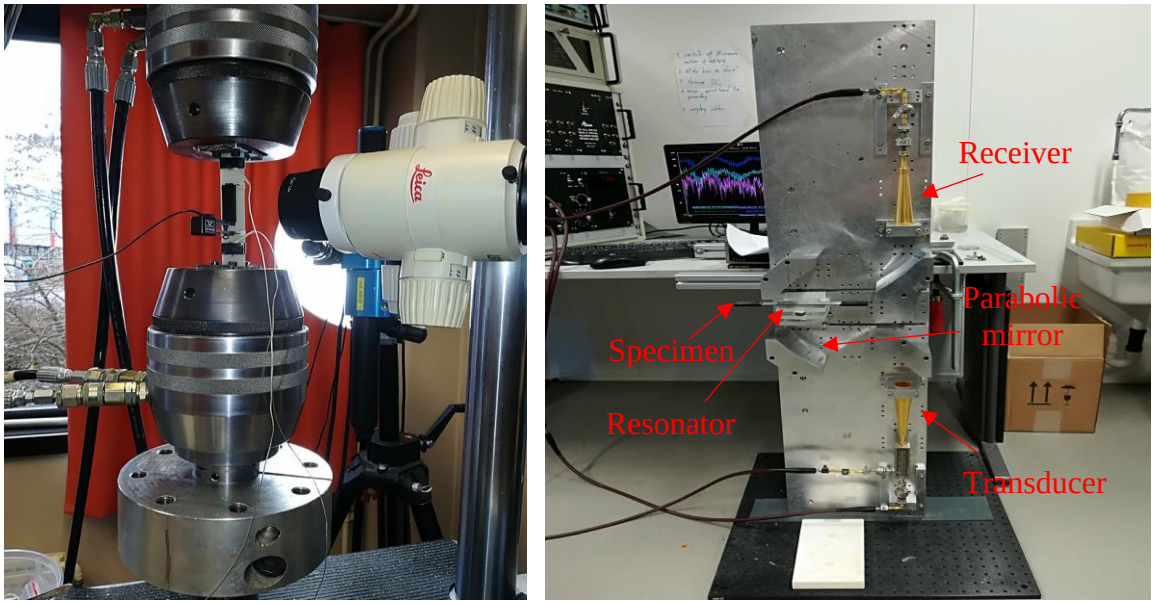

a) **b)**

Figure 1: a) Set-up used for testing and b) MMW equipment used

3. Results

Initially, static tests were performed without any interruptions in order to mechanically characterize the material and to have a general overview of the acoustic response during the whole static test captured by the AE equipment. From the initial static tests, the mechanical properties listed in Table 1 were obtained.

Table 1: Mechanical properties of the cross-ply laminates

Engineering constant	Unit	Value
$\sigma_{x,u}$	[MPa]	426.41
E_x	[GPa]	22.88
$\varepsilon_{x,u}$	[%]	1.92

The specimens at the initial static tests failed in a load equal to approximately 18 kN. According to this, static tests were then performed and interrupted for every 3 kN load increase in order to monitor the damage development during all these steps. Consequently, the static tests were performed and interrupted after 3, 6, 9, 12 and 15 kN applied load and the specimens were in every step unmounted off the machine to be scanned with the optical microscope and the MMW equipment.
In Figure 2, the total acoustic emission activity recorded during the static tests is plotted versus the total testing time. At the same graph, the stress increase during the static tests is plotted. The first conclusion made out of the static tests is that no acoustic emission hits are recorded until a stress equal to 85 MPa, which corresponds to 20% of the ultimate strength of the material. From this value on, an increase in the acoustic activity is recorded and at the same time, the stiffness of the material is decreased as revealed from a non-linearity in the evolution of the stress during the test. The reason for this increase in the acoustic activity response and the non-linearity in the stress-strain curve is obviously due to the appearance of the initial damage in the material. This damage can even be detected by using the DIC software.

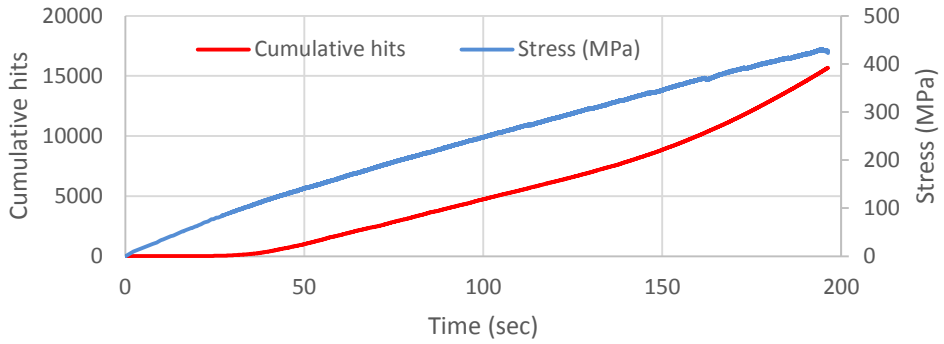

Figure 2: Evolution of the AE activity and the stress during static tests

In order to use the DIC results for an estimation of the damage, the σ value can be used. The σ value corresponds to the confidence interval for the match at any point of the analysed area compared to the reference picture in the unloaded situation and is measured in pixels. In Figure 3, the map of the σ value on the surface of the specimen is shown for three different loading conditions. Figure 3a) corresponds to a stress of 70 MPa at which according to the AE activity no damage is expected. Figure 3b) corresponds to a stress of 100 MPa at which the damage has almost started appearing and Figure 3c) to a stress of 330 MPa at which damage has developed. The analysed area from DIC corresponds to a total length of 50 mm. The DIC results are in total accordance with the AE activity and both of them estimate almost the same stress for the initiation of damage in the material.
We can notice that measurement of the crack density using the DIC software is possible. To be confident that the values measured with the DIC are reliable, measurements of the crack density were performed just with optical observation in every load step taking into advantage the transparency of the GFRP specimens. By this a conclusion was made that the crack density measured with the DIC and the optical observation were in total accordance.

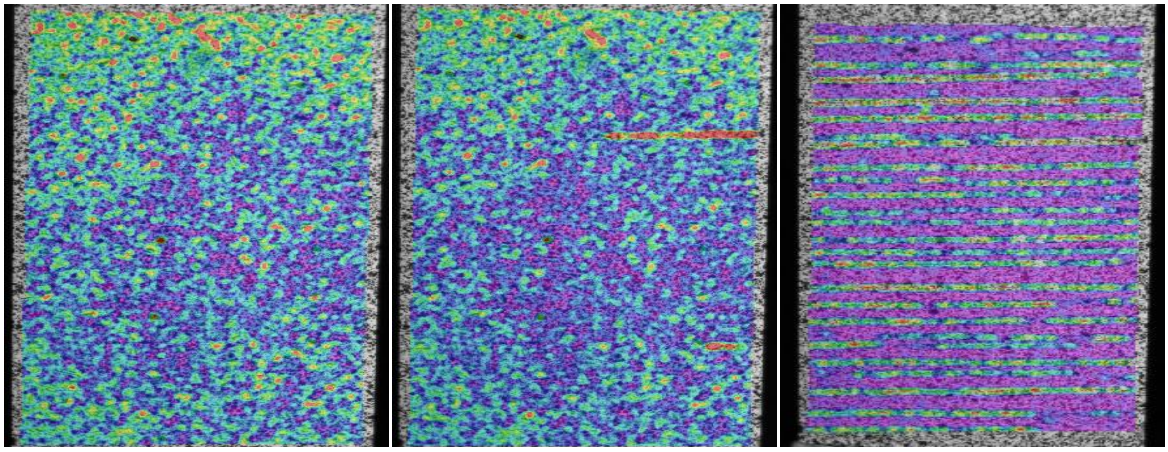

a) **b)** **c)**

Figure 3: σ value map obtained from DIC at a) 70 MPa, b) 100 MPa and c) 330 MPa stress

In Figure 4, the evolution of the crack density versus the stress is plotted. We can clearly see that the initiation of the damage as measured from the crack density is in good correspondence with the AE activity. In both cases, the initiation of the damage at a stress equal to approximately 20% of the ultimate strength is predicted. The crack density seems to increase with a high rate after this percentage and when a stress equal to 65% of the ultimate strength is reached, a saturated condition seems to appear for which the increasing rate of the crack density decreases.

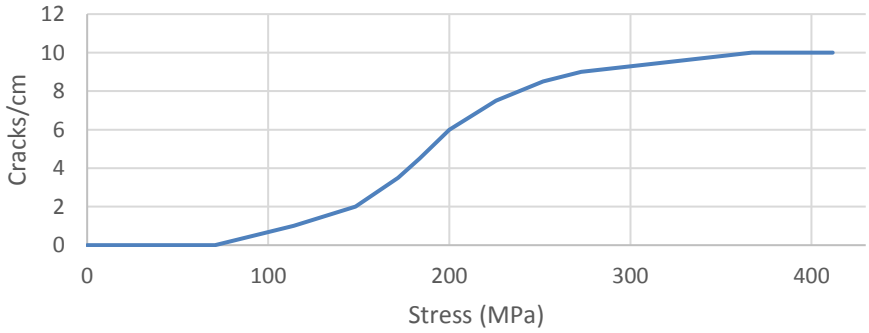

Figure 4: Evolution of the crack density as a function of the applied stress

However, this evolution of the crack density is not clearly shown from the AE results at least if only the cumulative acoustic signals recorded are taken into account. From the evolution of the cumulative hits we can observe a more or less linear increase of the acoustic response during testing. The reason behind this is that the total AE activity recorded can hide more information about different damage mechanisms and not only about the cracks formation which are observed from the DIC. Towards the end of the test, we can notice that the slope of the cumulative hits evolution increases a bit. This comes to an agreement with the through-thickness optical microscope observations. Specifically, after loading the specimen until 15 kN, delamination between the outer 90^o layers and the inner 0^o layers was evident, which was not evident after the load of 12 kN was applied. This reveals the appearance of another damage mechanism in the range of 12–15 kN loading, which is not obviously clear with the DIC software but can be reflected on the AE activity.

Considering now the results obtained from the MMW equipment, in Figure 5a) the reflection measured in the frequency range 50-70 GHz for the different load steps is presented whereas in Figure 5b) a zoom-in at around 61.5 GHz frequency is shown. Looking at Figure 5a), we can clearly see an increase in the reflected signal as the applied load increases. More specifically, after comparing the 3 kN load with the 15 kN load, a significant difference of almost 10 dB in the reflected signal is shown. The increase in the reflection is significantly higher in the range 3-6 kN and 6-9 kN, while an obviously smaller increase is measured in the load range 9-12 kN and 12-15 kN. This comes to a really good agreement with the saturation of the cracks observed in this load range 9-15 kN. If we look in more detail around the 61.5 GHz frequency at Figure 5b) we can clearly see the same tendency, together with the fact that the 9 kN and 12 kN steps almost coincide while a small increase of 2 dB in the reflection is shown for the load step of 15 kN, which is the range where delaminations have been observed.

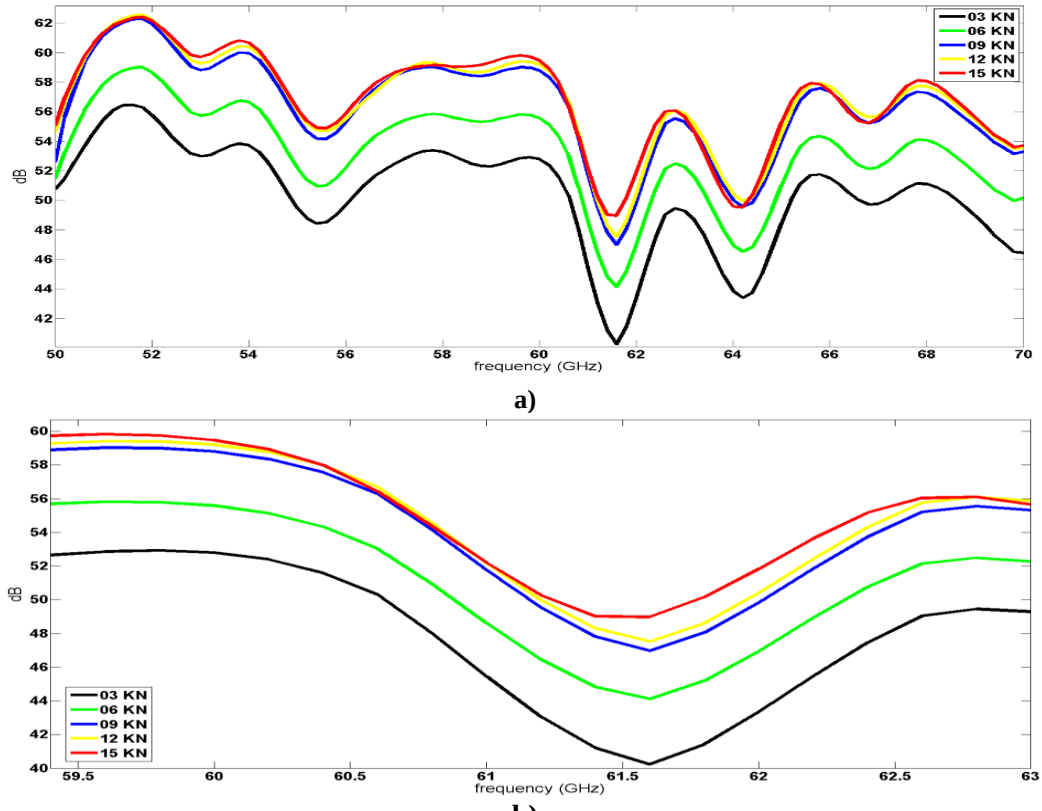

Figure 5: Measured reflection a) in the range 50-70 GHz electromagnetic radiation and b) around 61.5 GHz electromagnetic radiation

Looking now at the measured transmission of the emitted radiation, in Figure 6a) the change in the transmitted signal in the range 50-70 GHz is presented and in Figure 6b) a zoom-in around 51.5 GHz is plotted. What we clearly notice is an increase of almost 4 dB in the transmitted signal as the load increases from 3 kN to 15 kN. However, a clear differentiation in the amount of the transmitted signal between the steps after the 6 kN loading is difficult to be made. Only if we focus in the range of 51.5 GHz, an increase in the transmitted signal is evident as the load and consequently the damage increases. A basic conclusion that can be made is that an increase of the damage is more evidently resembled by an increase in the reflected radiation rather than in the transmitted one.

Moreover, the appearance of matrix cracks seems to lead to higher differences in the reflected and transmitted signal rather than the appearance of delaminations.

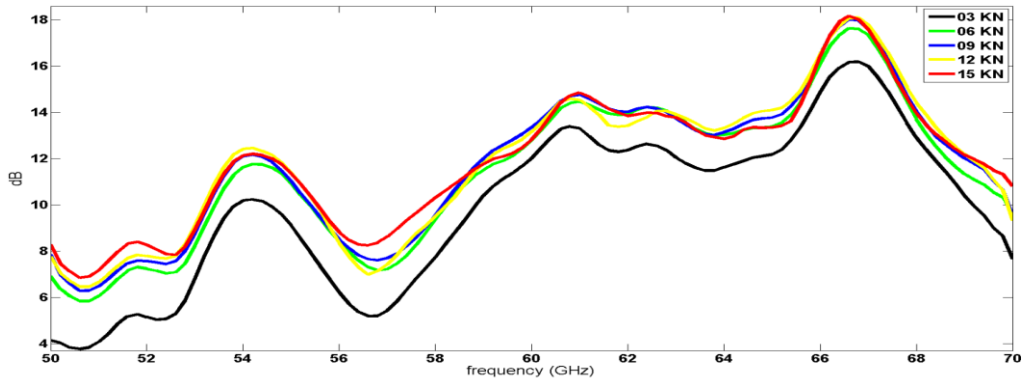

a)

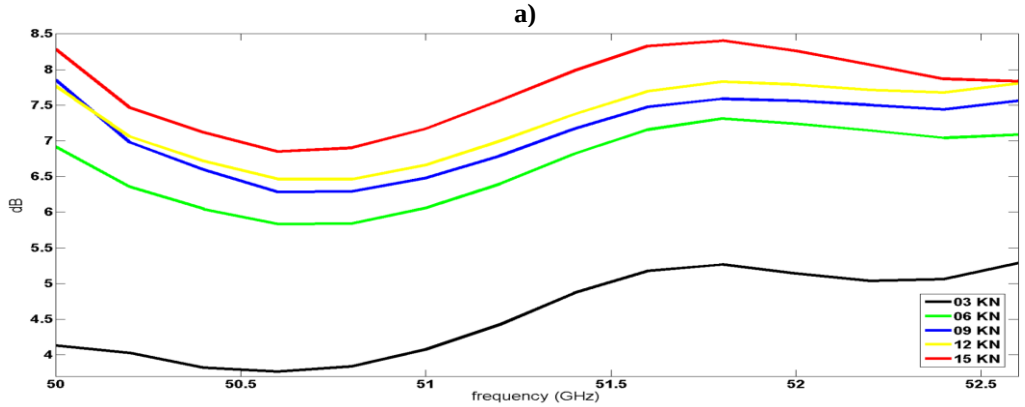

b)

Figure 6: Measured transmission a) in the range 50-70 GHz electromagnetic radiation and b) around 51.5 GHz electromagnetic radiation

4. Conclusions

In this study, different NDTs were combined so as to study the damage process in a cross-ply GFRP. The results from the static tests performed are quite promising. The AE software offers a more qualitative estimation of the damage process showing the transition of one damage mode to another. A detailed study of the features of the AE signals is necessary in order to characterize the signals developed by different damage modes. The AE results agree well with the damage monitored from through-thickness monitoring with an online microscope and with the cracks density measured from DIC. The MMW technique shows very interesting findings which correlate well with the previous results and offers a more quantitative estimation of the damage process. The development of damage seems to influence more the reflected signal rather than the transmitted one. However, both signals show an increasing tendency as the damage increases. A direct correlation of the increase in the reflected and the transmitted signal with the cracks density is possible. Finally, the increase of matrix cracks seems to influence more the reflected signal in relation to the appearance of delaminations since it results in bigger differences in the measured reflection.

Acknowledgements

The authors acknowledge the financial support of the FWO Research Funding Program "Multi-scale modelling and characterisation of fatigue damage in unidirectionally reinforced polymer composites under multiaxial and variable-amplitude loading". The authors of the ETRO department also acknowledge Vrije Universiteit Brussel for funding means through the SRP-project M3D2 and the IOF-ETRO project.

References

1. J Bohse, "Acoustic Emission examination of polymer-matrix composites", J. Acoustic Emission 22, pp 208-223, 2004.
2. AS Paipetis and DG Aggelis, "Damage assessment in fibrous composites using Acoustic Emission", Dr. Wojciech Sikorski (Ed.), InTech, chapter 13, 2012.
3. N Chandarana, DM Sanchez, C Soutis and M Gresil, "Early damage detection in composites during fabrication and mechanical testing", Materials 10, pp. 685-700, 2017.
4. P Nimdum and J Renard, "Use of acoustic emission to discriminate damage modes in carbon fibre reinforced epoxy laminate during tensile and buckling loading", ECCM15 Conf. Proc., 2012.
5. I Amenabar, F Lopez and A Mendikute, "In introductory review to THz Non-Destructive Testing of composite Mater", J. Infrared Millimeter and Terahertz Waves 34, pp 152-169, 2013.
6. A Pourkazemi, G Pandey, J Assaf, P Bismpas, E Tsangouri, J Stiens and D Aggelis, "Combination of Acoustic Emission and Millimeter Wave Spectroscopy techniques to investigate damage on cementicious materials", EAC2 Conf. Proc., pp 155-160, 2017.
7. C Jördens, M Scheller, S Wietzke, D Romeike, C Jansen, T Zentgraf, K Wiesauer, V Reisecker and M Koch, "Terahertz spectroscopy to study the orientation of glass fibres in reinforced plastics", Composites Science and Technology 70, pp 472-477, 2010.
8. C Ryu, S Park, D Kim, K Jhang and H Kim, "Nondestructive evaluation of hidden multi-delamination in a glass-fiber-reinforced plastic composite using terahertz spectroscopy", Composite Structures 156, pp 338-347, 2016.
9. G Dobmann, I Altpeter, C Sklarczyk and R Pinchuk, "Non-Destructive Testing with micro- and MMWs - Where we are - Where we go", Welding in the World 56, pp 111-120, 2012.
10. F Rutz, M Koch, S Khare, M Moneke, H Richter and U Ewert, "Terahertz quality control of polymeric products", Int. J. Infrared and Millimeter Waves 27, pp 547-556, 2006.
11. J Park, K Im, I Yang, S Kim, S Kang, Y Cho, J Jung and DK Hsu, "Terahertz radiation NDE of composite materials for wind turbine applications", Int. J. Precision Engineering and Manufacturing 15, pp 1247-1254, 2014.
12. T Chady, P Lopato and B Szymanik, "Terahertz and thermal testing of Glass-Fiber Reinforced Composites with impact damages", Sensors, 2012.
13. J Stiens, V Matvejev and G Pandey, "Enhanced characterization of dielectric properties" patent, EP 3156784 A1, 2017.